

# Thermal Study of an Iced Cable by the Finite Element Method

Dr. P. Fu and Prof. M. Farzaneh

NSERC/Hydro-Quebec/UQAC Industrial Chair on Atmospheric Icing of Power Network Equipment (CIGELE) and Canada Research Chair on Atmospheric Icing Engineering of Power Networks (INGIVRE) at the University of Quebec at Chicoutimi, Chicoutimi, Quebec, Canada,  
<http://www.cigele.ca>

**Abstract - In this paper, a FEM approach is proposed to evaluate the heat transfer and temperature gradient of a bare and an iced cable under icing conditions. It is a preliminary study for a project that is intended to calculate the conjugate heat transfer for an icing cable. The cable under consideration is current-carrying. The Finite Element Method (FEM) was used to solve the hybrid ice-aluminium domains that may be governed by the Poisson Partial Differential Equations (PDE). The boundary conditions for the dry- and wet-ice accumulations were prepared differently, i.e. the Neumann condition for the former, and the mixed Dirichlet-Neumann condition for the latter. In application, four sets of local heat transfer coefficients, respectively for low, medium and high levels of roughness from Achenbach's studies, and for a cable surface made of torsional strands, were taken as an input for the model boundary conditions so as to determine the optimum formula for cable icing. Also, the effects of wind speed and ambient temperature on the temperature of the cable were closely examined, which led to a number of conclusions. The validity and reliability of the method were confirmed partially by comparing the simulation results with those obtained from the experimental tests.**

## I. INTRODUCTION

In earlier days of icing researches (Lozowski *et al.* 1983, Makkonen 1984), the thermal exchange between the ice accretion surface and its substrate was ignored, and thus an adiabatic condition was assumed. Schilder (1987) made the first attempt to address this lack and proposed a calculation procedure to account for the internal heat conduction. For implementation, the cylinder and ice deposit were discretized into a number of isothermal elements that can be governed by the thermal diffusion equation. The finite-difference method was then used to solve the PDE system. However, this paper work stopped short of incorporating Joule heating although it may have been done easily with the same approach. At the same time, the question domain was discretized into a number of radial sections, a manner that suits well for a radial ice growth but which may impose restrictions for model application to an arbitrary ice shape. Jones (1996) took the

Joule heating into consideration by introducing the resistive heat flux directly in the heat-balance equations. This heat flux was assumed to dissipate evenly over the icing surface. It should be noted that, for a totally ice-covered cylinder, the method may be applied without risk of substantial error, whereas for a partially ice-covered cylinder, this method may cause a higher degree of inaccuracy, since the resistive heat flux under such a condition tends to show a great irregularity on the surface of the icing cylinder. Bouamoul (2002) proposed to use the FEM to calculate the temperature gradient of an ice-shedding cable. Again, as Joule heating was assumed to be negligible, it was possible to isolate and consider solely the ice accretion domain during modelling. It should be noticed that the current passing through the cable may be as high as 1000 Amps, which may cause the cable temperature to increase by 10~20 degrees with regard to the ambient temperature. As a result, the Joule heating can not be ignored in nowadays' modelling work. However, the inclusion of the internal heat transfer may complicate to a further degree the already complex modelling work (Fu, 2006). The reason is that modelling the conjugate heat transfer problem requires a coupling of the calculation procedures for the thermal process at the icing surface and the thermal process within the icing cable. The scope of the present work was limited to modelling the thermal process within an iced cable, for which the FEM is used to solve the Poisson domain composed of the cable and ice deposit. The FEM is believed to be an appropriate method here because the law of conservation of energy holds for any meshing element. A triangular mesh was created for the domain of interest because it ensures an excellent fit to any complex geometry. The number of triangular elements is determined as the result of a compromise between calculation efficiency and accuracy.

## II. BASIC PRINCIPLES

Figure 1 shows an energized cable that is covered asymmetrically by an ice deposit. The wind speed is  $u_0$ .

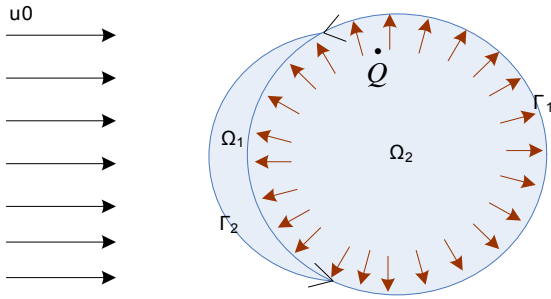


Fig. 1 An energized cable partially covered by ice deposit

In total, there are two calculation zones, one for the ice deposit and the other one for the energized cable. Both zones can be governed by the Partial Differential Equation of the same form, as follows:

$$-\nabla \cdot (k\nabla T) = \dot{Q} \quad (1)$$

or

$$-\nabla \cdot (k\nabla T) - \dot{Q} = 0 \quad (2)$$

For the ice domain,  $\Omega_1$ ,  $k$  is the thermal conductivity of ice and  $\dot{Q}$  is zero because no heat is produced.

For the cable domain,  $\Omega_2$ ,  $k$  and  $\dot{Q}$  are the thermal conductivity of aluminium and heat source, respectively.

Multiplying an arbitrary test function  $V$  and integrating on  $\Omega$  yields:

$$\int_{\Omega} (-\nabla \cdot (k\nabla T) - \dot{Q})Vd\sigma = 0 \quad (3)$$

Integrating by part yields

$$\int_{\Omega} (k\nabla T) \cdot \nabla Vd\sigma - \int_{\Gamma} \vec{n} \cdot (k\nabla T) \cdot Vds = \int_{\Omega} \dot{Q}Vd\sigma \quad (4)$$

Assume that  $\phi_1 \dots \phi_i \dots \phi_n$  form the basis for the solution space,  $V$ .

$$\int_{\Omega} (k\nabla T) \cdot \nabla \phi_i d\sigma - \int_{\Gamma} \vec{n} \cdot (k\nabla T) \cdot \phi_i ds = \int_{\Omega} \dot{Q}\phi_i d\sigma \quad (5)$$

where  $\vec{n} \cdot (k\nabla T)$  can be evaluated using the Neumann boundary condition:

$$\vec{n} \cdot (k\nabla T) = g - qT \quad (6)$$

If the radiation cooling and solar heating are ignored, the present problem involves the convective heat transfer only, i.e.  $q = C_f$  and  $g = C_f \times T_s$ .

$$\int_{\Omega} (k\nabla T) \cdot \nabla \phi_i d\sigma + \int_{\Gamma} qT\phi_i ds = \int_{\Omega} \dot{Q}\phi_i d\sigma + \int_{\Gamma} g\phi_i ds \quad (7)$$

Expanding  $T$  in the same basis of  $V$ , that is  $T(x) = \sum t_j \phi_j$ , yields

$$\sum (\int_{\Omega} (k\nabla \phi_j) \cdot \nabla \phi_i d\sigma + \int_{\Gamma} q\phi_j \phi_i ds) t_j = \int_{\Omega} \dot{Q}\phi_i d\sigma + \int_{\Gamma} g\phi_i ds \quad (8)$$

So for each triangular element, a linear shape function is derived, which can be used to evaluate the integral terms in the above equation while entailing no significant difficulties in numerical calculations. Then the element-based equations over the ice deposit and energized cable are assembled into a single set of system matrixes. By applying the boundary conditions and solving the equation system, it is possible to obtain the heat flux and temperature distributions anywhere in the domains.

#### Boundary conditions:

On the boundary,  $\Gamma_1$ , the Neumann condition is used, as follows

$$\vec{n} \cdot (k\nabla T) = h_c (T_a - T_s) \quad (9)$$

On the boundary,  $\Gamma_2$ , the boundary condition can be a Neumann or Dirichlet condition, depending on either a dry-icing or wet-icing condition involved. For the wet-icing conditions, the Dirichlet condition is applied:

$$T_s = 0 \quad (10)$$

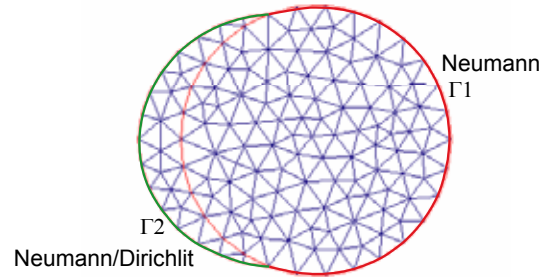


Fig. 2 Triangular mesh for Poisson domain

The heat generation due to the resistive or Joule heating may be expressed, in formulation, as follows:

$$Q_r = I^2 R_c / (\pi (D_c / 2)^2) \quad (11)$$

where the rated current,  $I$ , may be calculated according to the following formula:

$$I = (\text{Economical Current Density}) \times (\text{Conductor Cross-sectional Area}) \quad (12)$$

The conductor resistance,  $R_c$ , is a function of conductor temperature, and by referring to certain technical manuals, it is possible to obtain the resistances at both high and low temperatures,  $T_{high}$  and  $T_{low}$ , respectively. Consequently, the resistance at any particular temperature,  $T_c$ , may be obtained

by using linear interpolation according to the following equation:

$$R(T_c) = \left[ \frac{R(T_{high}) - R(T_{low})}{T_{high} - T_{low}} \right] \times (T_c - T_{low}) + R(T_{low}) \quad (12)$$

Suppose the cylinders under consideration are all 34.9 mm in diameter. The rated current for cables of this size is  $I = 860$  amp, and the electric resistance is  $R_c = 0.0625$  ohms/mile.

### III. SIMULATIONS AND RESULTS

As the first application of the calculation approach, a bare cylinder is considered and the Neumann boundary condition is applied. Since the cylinder has a smooth surface, the heat-transfer results from Achenbach's studies can be adopted. In total, three sets of local heat transfer coefficients were used, respectively for the low, medium and high levels of roughness. Figure 3 shows the heat transfer coefficients at an arbitrary angular position, obtained at  $ks/d = 75 \times 10^{-5}$ ,  $ks/d = 300 \times 10^{-5}$  and  $ks/d = 900 \times 10^{-5}$  for  $Re < 10^5$ .

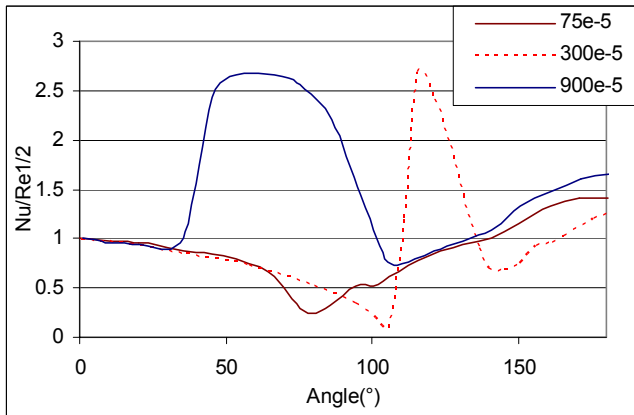


Fig. 3 Local Nusselt number regarding to its angular position

Figure 4 shows the temperature gradient for the above mentioned heat transfer coefficients. As far as the average temperature is concerned, the low-roughness case gives the highest temperature while the high-roughness case, the lowest temperature. Also, the cold zone is located on the windward side for the high-roughness case but is on the leeward side for the low-roughness case. This is due to the fact that high roughness promotes and engenders a turbulent boundary layer that leads to a higher average heat transfer rate, and that the maximum transfer rate appears at the windward direction. In such a case, heat is removed rapidly by convection, thus generating a large temperature drop. It should also be noted that the variations in temperature for these three cases are minor in magnitude because of the large thermal conductivity of the cylinder, that is, 220 W/m.K for aluminum.

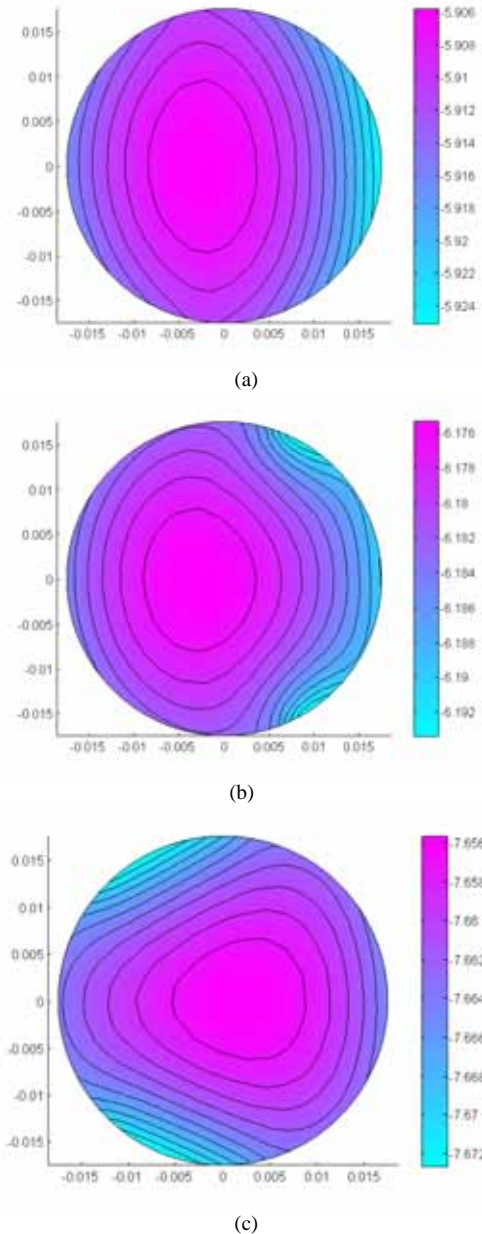


Fig. 4 Temperature distributions.  
 Roughness: (a)  $75 \times 10^{-5}$  (b)  $300 \times 10^{-5}$  (c)  $900 \times 10^{-5}$   
 Conditions: Air speed 5 m/s; Air temp.  $-10^\circ\text{C}$ ; Diameter 31.6 mm; Current 700 Amps

In order to validate the above mentioned calculation procedure, a series of experiments were carried out in the CIGELE Atmospheric Icing Research Wind Tunnel (CAIRWT). Figure 5 shows the current transformer, connections and experimental setup, which were used to generate the electrical current and measure temperature data.

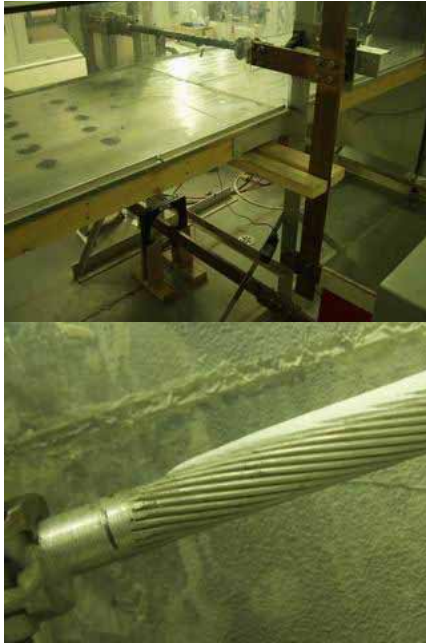


Fig. 5 Experimental set-up (a) Connections (b) test piece (cable)

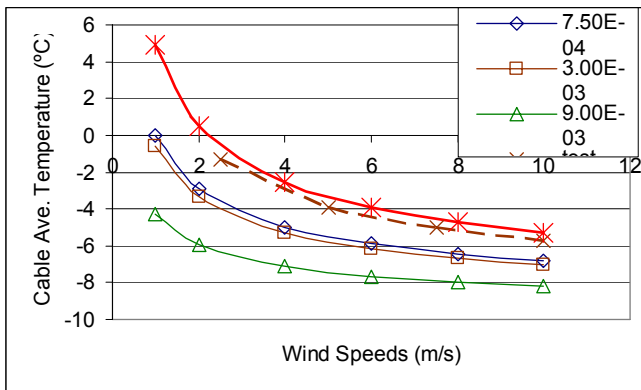


Fig. 6 Cable temperature versus wind speeds

Conditions: Air speed 5 m/s; Air temp. -10°C; Diameter 31.6 mm; Current 700 Amps

Figure 6 shows the curves generated from the calculated results and measured data, respectively. It is evident that the calculated results using Achenbach's data display a great discrepancy with the data obtained from experimental observations since a marked difference in average temperature can be observed in the figure. A further study reveals that the heat transfer coefficient from Achenbach (1977) could not be used for the cable made of torsional strands. That cable's unique structure dictates that its thermal conductivity and surface transfer rate differ greatly from those of an aluminum cylinder. Figure 7 shows the local Nusselt number obtained from numerical calculations (Péter 2006). By using the new Nusselt number, however, it is possible to obtain data that shows a striking agreement with the test data, as shown also in Figure 6. It was claimed in the same study that the thermal conductivity ranges from 3 to 12 W/mK, depending on the contact angle of the strands and the air gap inside.

Consequently, the differences in temperature over a cable cut can reach 1 degree, as proved experimentally in our test.

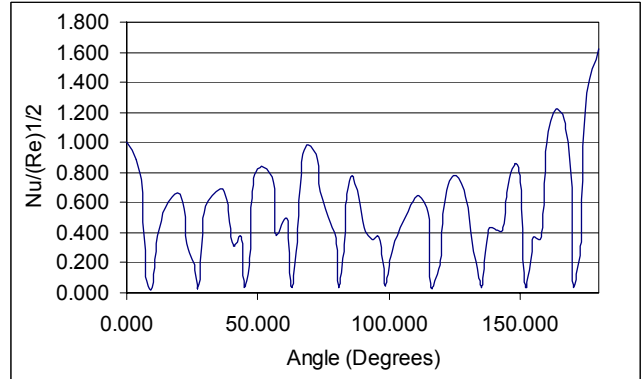


Fig. 7 Local Nusselt number regarding to its angular position for a cable

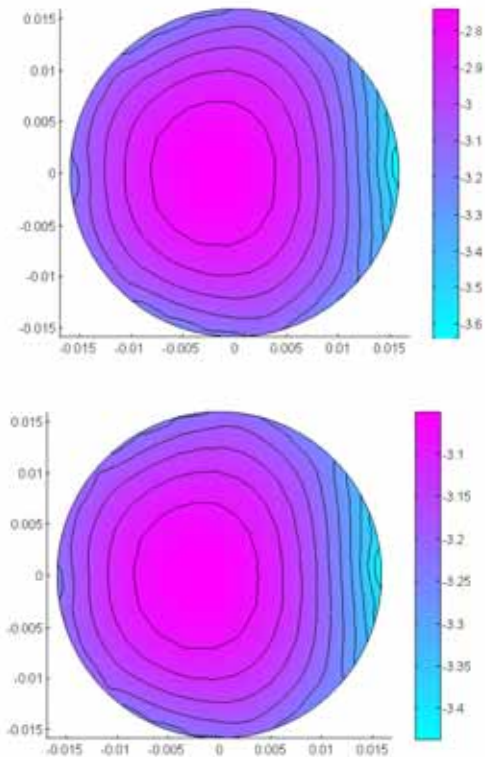


Fig. 8 Temperature Distributions (31.6 mm Cable, 700 Amps.

Thermal conductivity (a) 5 W/m.K (b) 12 W/m.K

Conditions: Air speed 5 m/s; Air temp. -10°C; Diameter 31.6 mm; Current 700 Amps

As mentioned earlier, the proposed FEM procedure can be used to calculate the heat transfer in multiple domains, that is, ice-cable domains. Figure 9 (a) shows the temperature profile for a dry ice accumulation whereas Fig. (b), for wet ice accumulation. As a result, the Neumann boundary conditions were applied in the former case. The lowest temperature appears at the stagnation point and the maximum temperature difference in the domain is up to 2°C. In the wet accumulation case, hybrid boundary conditions were applied accordingly; that is to say, the Dirichlet conditions were applied for the ice accretion surface while the Neumann conditions, elsewhere. It

is possible to observe that the lowest temperature appears on the leeward side and that the highest temperature appears in the middle of the cable. According to these two figures, it is possible to conclude that the temperature profiles for the dry- and wet- ice accumulations can be totally different.

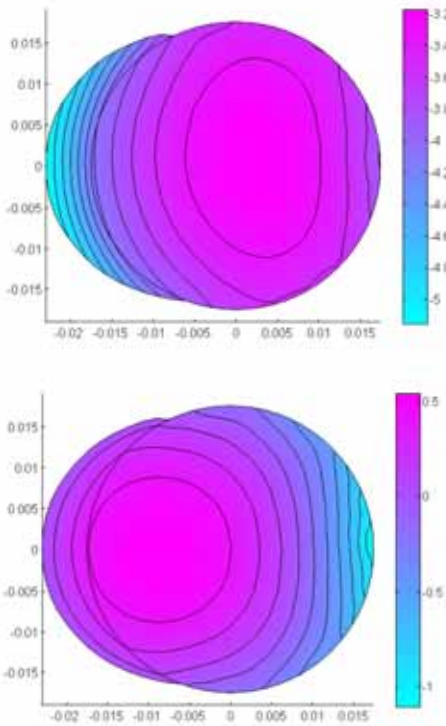


Fig. 9 Temperature Distributions

- (a) Temperature distribution for dry-ice accumulations
- (b) Temperature distribution for wet-ice accumulations

Conditions: Air speed 5 m/s; Air temp. -10°C; Diameter 35 mm; Current 860 Amps

It would also be interesting to know how the ambient temperature affects the cable temperature. Figure 10 shows that given the wind speed and current intensity, cable average temperature grows linearly with regard to ambient temperature. But the same conclusion can not be extended to the relationship between wind speed and cable temperature.

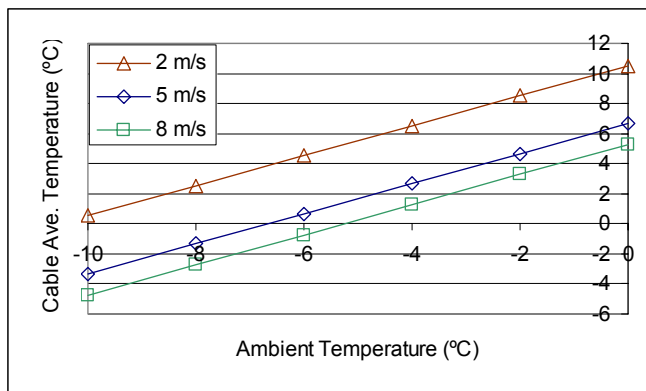


Fig. 10 Cable temperature versus ambient temperature  
Conditions: Diameter 31.8 mm; Current 700 Amps

The relationship of cable temperature vs. wind speed can be better displayed in Fig. 11, wherein three curves can be observed that represent the results for 0°C, -5°C and -10°C,

respectively. In general, this relationship can be represented by a polynomial curve. Cable temperature decreases rapidly with an increase in wind speed at the low-speed section, whereas the temperature decreases markedly at the high-speed section. This can be explained by the convective heat transfer occurring on the cable surface. The heat transfer rate is proportional to the square root of the Reynolds number and the Reynolds number varies linearly with regard to wind speed. Therefore, heat transfer rate is proportional to the square root of wind speed, which means that heat transfer increases rapidly at the low-speed section while the growth rate slows down at the high-speed section.

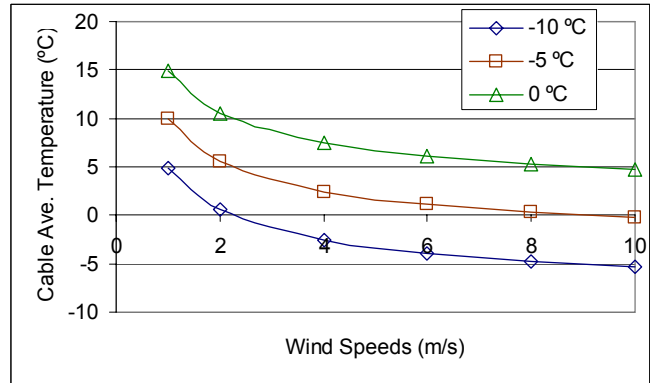


Fig. 11 Cable temperature versus wind speeds  
Conditions: Diameter 31.8 mm; Current 700 Amps

#### IV. CONCLUSIONS

The FEM was successfully applied to evaluate the heat transfer and temperature gradient of a bare and an iced cable under icing conditions. Through this study, it was found that such key parameters as the convective heat transfer coefficient and thermal conductivity should be estimated specifically for the type of cable under consideration. Otherwise, a substantial error may result. Therefore, it is recommended in future studies to take into consideration the heat flux due to evaporation and phase change. As such, the calculation procedure described herein may possibly be incorporated into an icing model.

#### V. ACKNOWLEDGEMENTS

This work was carried out within the framework of the NSERC/Hydro-Quebec/UQAC Industrial Chair on Atmospheric Icing of Power Network Equipment (CIGELE) and the Canada Research Chair on Engineering of Power Network Atmospheric Icing (INGIVRE) at Université du Québec à Chicoutimi. The authors would like to thank the CIGELE partners (Hydro-Québec, Hydro One, Électricité de France, Alcan Cable, K-Line Insulators, CQRDA and FUQAC) whose financial support made this research possible. The authors would like to thank Mr C. Zhang for his participation in some of the experiments.

## VI. REFERENCES

- [1] Bouamoul, A., "Processus de délestage naturel des câbles et conducteurs de transport d'énergie électrique", Ph.D. in Engineering, UQAC, 2002.
- [2] Fu, P., Farzaneh, M., Bouchard, G., "Two-Dimensional Modelling of the Ice Accretion Process on Transmission Line Wires and Cables". Cold Regions Science and Technology, vol. 46, no. 3, pp.132-146, 2006.
- [3] Jones, K. F., "Ice Accretion in Freezing Rain", Cold Regions Research & Engineering Laboratory, CRREL Report 96-2, 1996.
- [4] Lozowski, E. P., Stallabrass, J. R., and Hearty, P. F., "The Icing of an Unheated, Non-rotating Cylinder, Part I: A Simulation Model", Journal of Climate and Applied Meteorology, Vol. 22, pp. 2053-2062, 1983.
- [5] Makkonen, L., "Modelling of Ice Accretion on Wires," Journal of Climate and Applied Meteorology, Vol. 23, No. 6, pp. 929-939, 1984.
- [6] Péter, Z., "Modelling and Simulation of the Ice Melting Process on a Current-Carrying Conductor", Ph.D. in Engineering, UQAC, 2006.
- [7] Szilder, K., Lozowski, E. P., and Gates, E. M., "Modelling Ice Accretion on Non-Rotating Cylinders –The Incorporation of Time Dependence and Internal Heat Conduction ", Cold Regions Science and Technology, Vol. 13, pp. 177-191, 1987.